In-Situ Detection of Small Biomolecule Interactions Using a Plasmonic Tilted Fiber Grating Sensor

Xiaoyong Chen, Yinggang Nan, Xuanyue Ma, Haiyang Liu, Wei Liu , Lei Shi ,
and Tuan Guo , *Senior Member, OSA*

Abstract—We have proposed and experimentally demonstrated a plasmonic tilted fiber Bragg grating based biosensor for *in-situ* detection of the small biomolecule S-adenosyl-L-homocysteine (AdoHcy). The sensor can also monitor the molecule's interaction with the protein Set7 in real time. The biosensor is made by coating a 50-nm-thick gold film over an 18° tilted fiber Bragg grating. A spectrally dense comb of backward-propagating cladding resonance modes with Q-factor as high as 10^4 is excited due to the tilted grating. The spectral overlap between the excited cladding modes and the broader absorption feature of the surface plasmon makes this device a unique tool for high-accuracy measurement of small shifts of plasmon resonance wavelength. Surface biomolecular functionalization of the gold film enables us to not only detect the corresponding biomolecule but also study its interaction with other biomolecules. Our experimental results demonstrate that our biosensor can detect AdoHcy at concentration as low as 1 nM. Furthermore, we have successfully real-time monitored interaction between the protein Set7 and AdoHcy at different concentrations. Our measurements are consistent with the biological theory that the association rate of a pair of biomolecules depends on their concentrations.

X. Chen was with the Institute of Photonics Technology, Jinan University, Guangzhou 510632, China. He is now with the Department of Physics, Shantou University, Shantou 515063, China (e-mail: xychen1986@126.com).

Y. Nan and T. Guo are with the Guangdong Provincial Key Laboratory of Optical Fiber Sensing and Communications, Institute of Photonics Technology, Jinan University, Guangzhou 510632, China (e-mail: yinggangnan@qq.com; tuanguo@jnu.edu.cn).

X. Ma and L. Shi are with the JNU-HKUST Joint Laboratory for Neuroscience and Innovative Drug Research, Jinan University, Guangzhou 510632, China (e-mail: 578012254@qq.com; sophielshi80@gmail.com).

H. Liu is with the Shenzhen Key Laboratory for Neuronal Structural Biology, Shenzhen Peking University–The Hong Kong University of Science and Technology Medical Center, Shenzhen 518036, China, and also with the Division of Life Science, State Key Laboratory of Molecular Neuroscience, The Hong Kong University of Science and Technology, Clear Water Bay 87P8+H5, Hong Kong (e-mail: liuhy@ust.hk).

W. Liu is with Shenzhen Key Laboratory for Neuronal Structural Biology, Shenzhen Peking University–The Hong Kong University of Science and Technology Medical Center, Shenzhen 518036, China (e-mail: liuwei@sphmc.org).

Color versions of one or more of the figures in this paper are available online at http://ieeexplore.ieee.org.

Digital Object Identifier 10.1109/JLT.2018.2870337

Index Terms—Surface plasmon resonance, optical fiber sensor, tilted fiber Bragg grating, biomolecule interaction.

I. INTRODUCTION

DUE to many well-known desirable features such as small size, cost-effectiveness, biocompatibility and multiplexing ability, fiber-optic devices have been increasingly employed as biomedical sensors for label-free biosensing in recent years [1]–[4]. Fiber-optic biosensors be easily inserted into the media, instead of having to bring samples to an instrument. Such sensors make it possible to collect measurements *in-situ* and remotely. Among fiber-optic sensor types, the tilted fiber Bragg grating (TFBG), in which the refractive index (RI) modulation planes are tilted by several degrees relative to the propagation axis, has attracted increased attention owing to its ability to inexpensively and quickly measure very small changes in the surrounding refractive index of the fiber [5], [6].

TFBGs can be ultraviolet-inscribed in the cores of optical fibers without any gross mechanical modification to the fiber structure. The tilted grating breaks the cylindrical symmetry of the fiber, thereby coupling some of the core-guided light into lossy modes travelling backwards in the cladding. The cladding mode resonances can be observed as a comb of sharp dips in the transmission spectrum, covering a wavelength band, typically tens of nanometers wide, on the short wavelength side of the core Bragg resonance (also called core mode). The symmetry breaking also results in strong polarization selectivity of the excited cladding modes induced by the TFBG. The cladding modes can excite surface plasmon resonances (SPRs) in a thin metal coating covering the cladding. The SPRs damp some of the cladding mode resonances, whose effective mode refractive indices are determined by the grating geometry. The transmitted spectrum is very sensitive to surrounding refractive index matching the effective mode indices of the resonances. The quality factors (Q-factors) of the resonances can be as high as 10^4, enabling accurate measurement of small shifts in resonances. Such a metal-coated TFBG, which is also called a plasmonic TFBG or TFBG-SPR, can meet the requirement of low limit of detection (LOD) in biomedical and biochemical sensing applications [7]–[10].

In comparison with the conventional TFBG without a metal coating, plasmonic TFBGs have several advantages: the surface plasmon polariton (SPP) propagating at a metal-dielectric interface is very sensitive to the change of RI near the metal surface

because of the large localization of electromagnetic energy in the layer immediately adjacent to the metal surface. Therefore, any perturbation near the metal layer, such as the bonding of analytes on receptor molecules, can potentially be sensed by a plasmonic TFBG sensor [11], [12]. Plasmonic TFBG sensors open up a multitude of opportunities for single-point biomedical sensing in hard-to-reach spaces, and offer a greatly improved LOD for molecular interactions together with very controllable cross-sensitivities.

Methylation is significant in epigenetic regulation of protein expression via deoxyribonucleic acid and histone methylation. S-adenosyl-L-homocysteine (AdoHcy) is the product of all methylation reactions that involve S-adenosyl-L-methionine (AdoMet) as the methyl donor, and is the immediate precursor of all of the homocysteine produced in the body [13]. The inhibition of these AdoMet-mediated processes by AdoHcy is a proven mechanism for metabolic alteration. As the conversion of AdoHcy to homocysteine is reversible, with the equilibrium favoring the formation of AdoHcy, increase in plasma homocysteine is accompanied by an elevation of AdoHcy concentration in most cases. Disturbances in the transmethylation pathway indicated by abnormal AdoHcy, AdoMet, or their ratio have been reported in many pathological conditions, including dementia, depression, Parkinson's disease, allergic disease, congenital abnormalities, cardiovascular disease and certain malignancies [14], [15].

Recent research suggests that AdoHcy-mediated hypomethylation provides an alternative mechanism for the pathogenesis of diseases related to hyperhomocysteinemia [16]. Furthermore, many studies have shown that AdoHcy is a critical factor for cardiovascular disease [17], [18]. Hence, a fast, sensitive, and precise analytical method for the determination of AdoHcy is required to evaluate clinical conditions.

Several methods have been developed for the detection of AdoHcy in tissues and body fluids. For example, liquid chromatography combined with ultraviolet detection is frequently used for AdoHcy (concentration in micromolar range) measurement in tissue and red blood cells [19], [20]. In plasma and cerebrospinal fluid, however, the AdoHcy concentration is considerably low, typically 10 to 100 nmol/l [21], resulting in difficult measurement. Thus, a more sensitive detection is required. Liquid chromatography-based methods [22], [23] that enable detection in the nanomolar range were proposed to detect AdoHcy in plasma and cerebrospinal fluid. But these methods have disadvantages of high-cost due to the need for expensive equipments, and difficult implementation. An current method like capillary electrophoresis [24] was also proposed for AdoHcy measurement. This method simplifies the operation process and shortens the measured time, but it is at the price of large sample solution. Last but not least, enzyme linked immunosorbent assay method [25] was studied in recent years owing to its merits of label-free detection and ability to study the affinity between AdoHcy and the corresponding anti-AdoHcy antibody. However, this method has some pronounced drawbacks like time-consuming and requirement of large sample solution. Hence, to quickly, cheaply and accurately measure AdoHcy concentration in body fluids and tissue, new sensing techniques

with high sensitivity, but using label-free methods in small scale point-of-care devices is must be developed.

In this work, we propose and experimentally demonstrate a label-free detection of the small biomolecule, AdoHcy, using a plasmonic TFBG sensor. The biosensor is designed as a reflective probe type with a 50-nm-thick gold film coating over the cladding surface of an 18° TFBG, together with a surface functionalization with protein lysine methyltransferase Set7 acting as the bio-receptor. The sensor is fabricated without any damage to the fiber's structural integrity, thereby ensuring the stability and reproducibility of the sensor. Moreover, using a custom-designed microfluidic system, we not only demonstrate AdoHcy detection, but also monitor in real-time the interaction between AdoHcy and protein Set7 in microliter sample volumes.

II. MATERIALS AND METHODS

A. Materials

The AdoHcy (with concentration of 35 mM, supplied in a 1-ml centrifuge tube) and protein lysine methyltransferase Set7 (with concentration of 560 μM, stored in a 1-ml centrifuge tube) were provided by Dr. Wei Liu (Shenzhen Peking University-The Hong Kong University of Science and Technology Medical Center, Shenzhen, China). These two samples were stored in a freezer at -80 °C prior to use. The 11-Mercaptoundecanoic acid (MUA) that we used to connect the bio-receptor (protein Set7) to the surface of the gold film, and the 1-ethyl-3-(3-dimethylaminopropyl) carbodiimide hydrochloride (EDC) and N-hydroxysuccinimide (NHS) we used for activating the carboxyl provided by the MUA were purchased from Wuhan Boster Biological Engineering Co., Ltd, Wuhan, China. They were stored in the fresh food compartment of a domestic fridge at 4 °C prior to use.

B. Plasmonic Tilted Fiber Grating Fabrication

The TFBG was fabricated in commercial single-mode fiber using the phase-mask technique. Prior to grating inscription, the fiber was hydrogen loaded at a temperature of 50 °C, at a pressure of 1500 psi for 168 h, to increase the photosensitivity of the fiber core. Then we cylindrically focused a 193 nm pulsed ultraviolet light from an ArF excimer laser, using a power of 3 mJ per pulse and frequency of 200 Hz, through the ± 1 diffraction order phase-mask and onto the fiber. By spatially scanning the beam over the fiber region, we inscribed gratings at the desired tilt angle into the fiber core within a very short length (< 2 cm), as shown in Fig. 1. The phase mask was angled to select the tilt angle of the grating's refractive index planes in the fiber. In this work, we selected an TFBG with tilt angle of 18°, which provides the maximum amplitude of cladding modes for measuring RI in the range 1.30 to 1.38 in aqueous solutions [26].

A 50-nm-thick gold film was radio-frequency magnetron sputtered (model TRI-S500 fiber material metal coating system, Changchun Institute of Optics, Fine Mechanics and Physics) onto the fiber over a 2 to 3-nm thick film of chromium. The chromium film served to increase adhesion between the gold and the fiber. The chromium film was coated on the fiber using
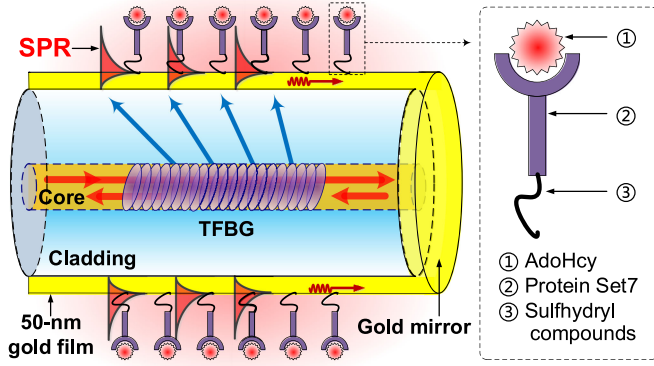
Fig. 1.　Detail of the TFBG-SPR sensor with the process of specific surface functionalization.

the same method as the gold film. Film uniformity was maintained by rotating the fiber about its axis at 0.5 rad/s during the deposition process. A gold mirror was deposited on the end of the short fiber containing the TFBG to make the probe operate in reflection.

The gold coated TFBG is shown in Fig. 1, together with the working principle. The blue arrows represent light resonantly coupled from the core of the single mode fiber to a multitude of modes propagating in the cladding, each at a resonant wavelength corresponding to an effective mode index. When the axial component of the propagation constant of the cladding mode equals that of an SPP, coupling to that SPP can occur and the transmission spectrum of the TFBG reveals a consequent reduction in the light intensity.

The working principle of the proposed TFBG sensor can be described as the following two equations [27], [28]:

$$\lambda_{clad,i} = \left(N_{clad,i}^{eff} + N_{core}^{eff} \right) \Lambda \qquad (1)$$

$$\beta_{SPP} = \frac{\omega}{c} \sqrt{\frac{\varepsilon_m \varepsilon_s}{\varepsilon_m + \varepsilon_s}} \qquad (2)$$

The cladding modes (resonance dips) excited in the fiber cladding are decided by the phase match condition of eq. (1), where N_{core}^{eff} and $N_{clad,i}^{eff}$ are the effective indices of the input core mode and excited cladding mode with the order of i, respectively; Λ is the period of the grating (measured along the fiber axis), c is the speed of light in vacuum, ω is the angular frequency of the light; ε_m and ε_s are the complex relative permittivities of the metal film and the surrounding material (including binding surface species and bulk solution) adjacent to the metal interface where the SPP is located, respectively. When $\beta_{SPP} = \beta_{clad,i} = \omega \cdot N_{clad,i}^{eff}/c$, combined with a proper polarization control, SPR can be achieved. Therefore, any perturbations near the metal layer, such as the bonding of analytes on receptor molecules, can be detected by measuring the power changes of the matched cladding modes.

C. Surface Functionalization

Following gold deposition the sensing probe was thoroughly rinsed with ethanol and with Milli-Q ultrapure water to remove

unwanted contaminants. Prior to the binding of the AdoHcy, the sensor was immersed in a solution of MUA in ethanol at a concentration of 2 μM for 12 hours, resulting in a self-assembled monolayer of mercapto compounds on the surface of the gold film, as shown in Fig. 1. Then the sensor was rinsed with ethanol and with Milli-Q ultrapure water to remove the unconnected MUA. Then the sensor was immersed in a mixture of 200 μl of NHS (180 mg/ml) and 200 μl of EDC (23 mg/ml) for 30 min. Next, the sensing probe was rinsed several times with a reaction buffer consisting of 50 mM of Tris-HCL and 100 mM of NaCl, with pH of 7.5. Finally, the sensing probe was immersed in the solution of protein Set7 with concentration of ∼5 μM for 2 hours to bind the protein Set7 to the self-assembled monolayer of mercapto compounds. After the binding of protein Set7, the biosensor was ready to detect the AdoHcy. Note that the protein Set7 binding to the surface was implemented using the microfluidic system described in Section III-B.

III. EXPERIMENTAL SYSTEM

A. Experimental Setup

Figure 2 presents the experimental sensing system. A broadband source (BBS) followed by a linear polarizer was the light source. The polarization state of the light launched into the TFBG sensor was controlled by a polarization controller (PC) which was adjusted to maximize the coupling of the excited cladding modes to the SPR, ensuring the strongest signal-to-noise ratio. A circulator was used to receive the light reflected from the gold mirror of the sensor, and the reflection spectra from the sensor were monitored and recorded by an optical spectrum analyzer (OSA) with a resolution of 0.02 nm.

B. Microfluidic System

Due to very limited available volumes of AdoHcy and Set7 solutions, it was impossible to detect the target molecules using the conventional method of fixing the biosensor in a vertical fiber clamp and immersing it in the targeted biosample solution held in a centrifuge tube placed on a variable height platform [29]. To functionalize the bio-receptor of protein Set7 on the gold film surface and detect AdoHcy, whilst using only microliter volumes of solutions, we employed a microfluidic delivery system, as shown in Figs. 2 (block diagram) and 3 (experimental system). A 2-channel microfluidic syringe pump (Model: NE-4000, New Era Pump Systems Inc.) with infusion rates from 1.436 μl/hr (1 ml syringe) to 7515 ml/hr (60 ml syringe) was employed for injecting biosample and buffer solutions automatically into the sample cell. For this work, the infusion rate was set to 2 μl/min. A glass capillary with inner diameter of 300 μm was used as the sample cell, and one end of it was connected, through a "Y" connector and silicone tubes (inner diameter of 350 μm), to both syringes fixed on the 2-channel syringe pump. The plasmonic TFBG biosensor was inserted into the capillary from the other end. The total solution volume for filling the sample channel (Channel 1 in Fig. 3) and sample cell is less than 20 μl. Therefore, this microfluidic system can provide biosample detection in microliter range for our proposed plasmonic TFBG
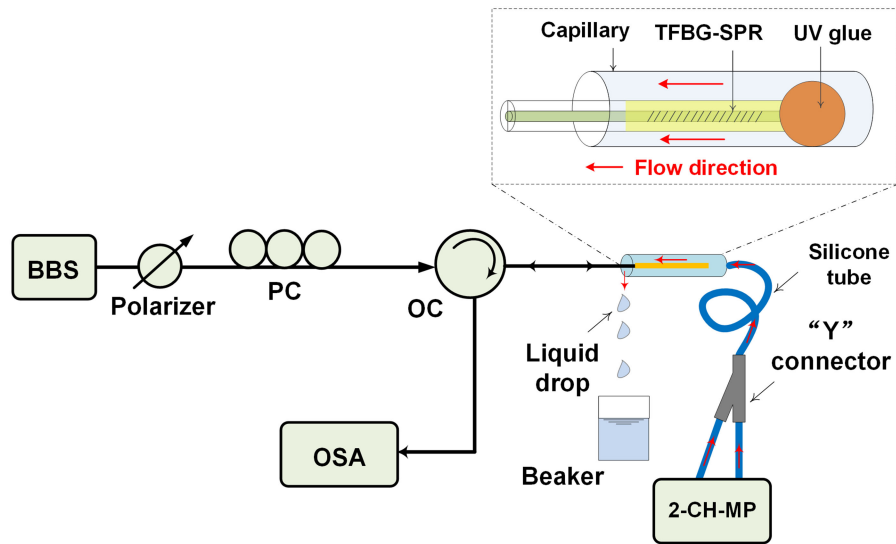
Fig. 2. Block diagram of experimental system. PC: polarization controller, OC: optical circulator, BBS: broadband source, OSA: optical spectrum analyzer, 2-CH-MP: 2-channel microfluidic pump, UV glue: Ultraviolet glue.
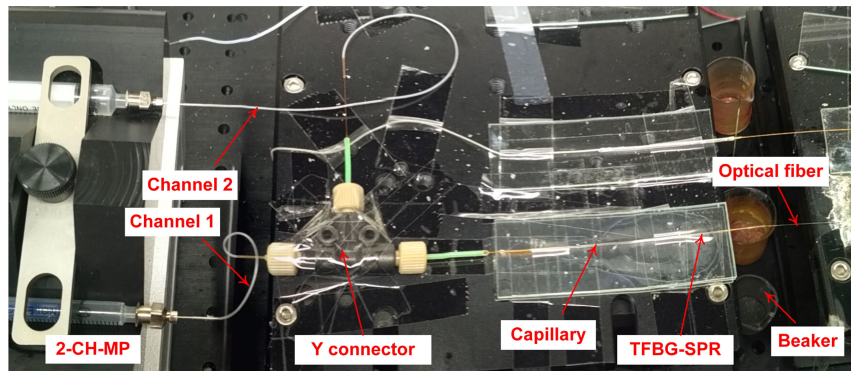

Fig. 3. Photograph of microfluidic sensing system.

biosensor. In addition, the microfluidic system makes it easy to monitor the interaction between the small molecule AdoHcy and the protein Set7.

C. Sensor Interrogation

Figure 4 shows a typical measured spectrum of the plasmonic TFBG sensor when immersed in buffer or sample solutions used in this work. Two spectral regions were studied during biosample measurement: For sensing biomolecules, we monitored the cladding mode resonance near 1491 nm, indicated with the blue star (see also inset (a)). For calibrating temperature-induced cross-sensitivity correcting for source intensity variations we monitored the core mode resonance near 1551 nm (see also inset (b)). The inset (a) clearly indicates that even a very small surrounding RI perturbation ($\Delta n \sim 10^{-4}$) could induce significant change in the SPR mode resonances. Observing the real-time spectral change, we found that the SPR modulated cladding modes (labelled "Selected SPR mode" in Fig. 4) clearly show an intensity variation induced by a small RI change of Δn, even though the corresponding wavelength shift is quite small. For maximum sensitivity we selected the signal at the minimum

of the cladding resonance dip located just to left (the shorter wavelength side) of the SPR attenuation maximum as our signal output, as indicated by the blue star in Fig. 4. Although the surrounding RI changes can arise from either bulk medium changes or from molecular binding events for functional layers attached to the metal surface, in this work only the latter occurs, because the RI of the bulk medium remains almost constant under the low concentration conditions.

The inset (b) in Fig. 4 shows that the core mode is insensitive to surrounding RI. Spectral shifts due to temperature changes can be eliminated by referencing all wavelengths to the core mode wavelength identified at the start of the experiment.

IV. RESULTS AND ANALYSIS

Based on the proposed biosensor and microfluidic system, two main experiments were performed, namely specific detection of small molecule AdoHcy, and detection of the interaction between AdoHcy and protein Set7.

Figure 5(a) presents the real-time spectral response of the selected cladding resonance after the sensor was immersed in
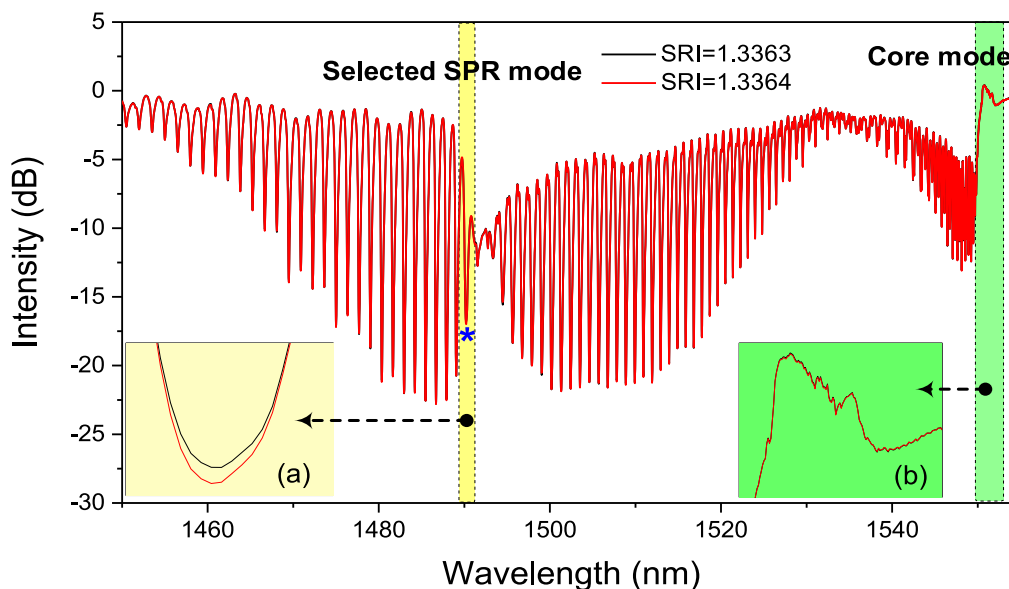
Fig. 4.   Reflection spectra from the TFBG-SPR sensor: (a) enlarged detail of the SPR mode resonance selected for sensing; (b) enlarged detail of the core Bragg mode.
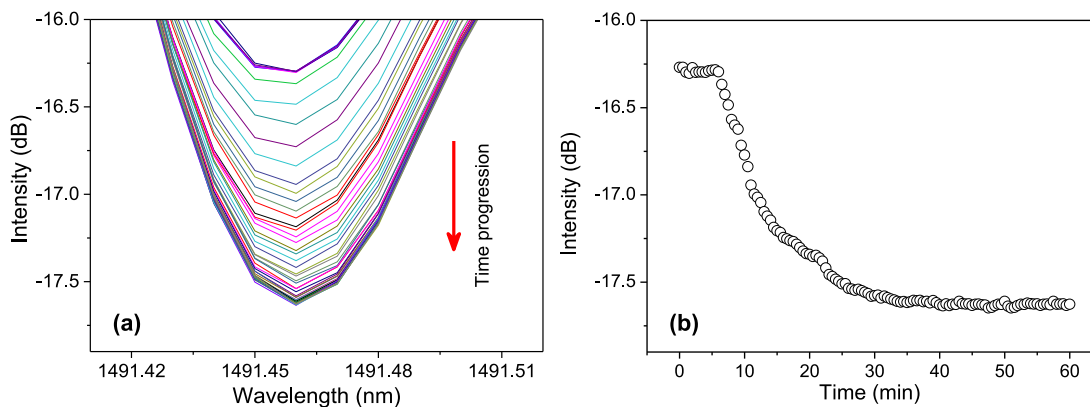

Fig. 5.   (a) Intensity response of the selected resonance versus protein Set7 functionalization, and (b) the corresponding intensity change over the whole time period.

the Set7 solution for functionalization of the sensor surface. As can be seen, the strength of the selected resonance changes with the time and finally stabilizes. The intensity at the center of the selected resonance versus time is plotted in Fig. 5(b). The intensity decreases rapidly during the first 20 minutes and then more slowly. The intensity becomes more or less stable after the sensor has been immersed in the protein Set7 solution for 35 minutes. The trend of intensity change can be understood as follows: When the RI near the metallized surface of the sensor increases, the SPR wavelength band moves slightly to the longer wavelength side, resulting in the selected cladding resonance, which is located just to left of the center of the SPR resonance feature, becoming deeper. This indicates that the protein Set7 has been successfully bonded to the sensor surface. Fig. 6, taken by microscope, shows the changes in the sensor's surface at different experimental stages. We can see that the surface roughness is clearly changed when the protein

Set7 is bonded to the surface (Fig. 6(c)). The surface roughness with AdoHcy bonded to Set7 (Fig. 6(d)) is almost the same as Fig. 6(c). This can be understood that the molecular weight of AdoHcy is only 384 Da, much smaller than the Set 7 (41 kDa). Therefore, the surface roughness affected by AdoHcy can be ignored when compared with that affected by Set7.

A. AdoHcy Detection

Figure 7 details the experimental result of AdoHcy detection at 1 nM concentration using the protein Set7-coated plasmonic TFBG biosensor. The plotted points are each the average of 5 repetitions of the experiment. From the figure we can see that as soon as the functionalized sensor is immersed in the 1 nM test solution, AdoHcy causes an intensity change which saturates after about 12 minutes. After biosensor immersion in the AdoHcy solution for about 12 min, the output of the biosensor
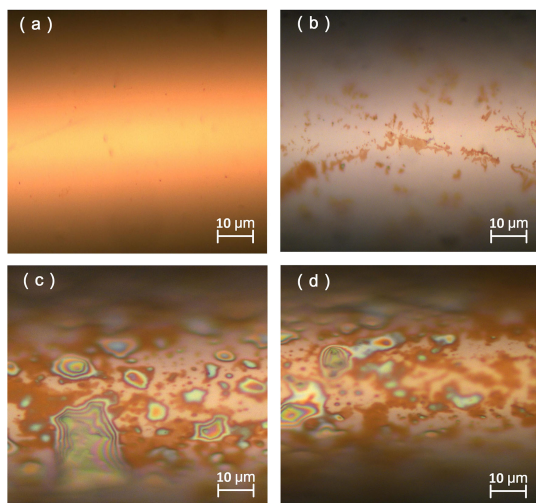
Fig. 6. Surface structure of the gold film under microscope at different experiment stages: (a) without any functionalization; (b) after immersion in MUA for 12 h; (c) after binding of the protein Set7; (d) after AdoHcy detection.
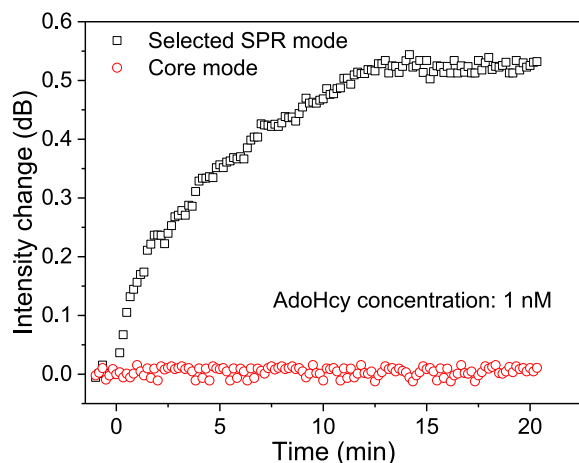

Fig. 7. Experimental results of AdoHcy detection at a concentration of 1 nM. The black squares represent the selected cladding resonance for AdoHcy measurement, and the red circles represent the monitoring of the core mode.

remains constant, with signal intensity about 0.5 dB lower than in the initial state. We have also carried out experiments with AdoHcy concentration (0.5 nM) lower than 1 nM. The measured intensity change was relatively small (< 0.1 dB) and unstable. Therefore, it can be concluded that the LOD of our biosensor based on Set7 functionalization over the metal layer for Ado-Hcy measurement is approximately 1 nM, which is one order smaller than the normal AdoHcy concentration in body fluid or tissue (10 ∼100 nM). Additionally, this LOD is also much smaller than that provided by capillary electrophoresis method (60 nM) [24] and enzyme linked immunosorbent assay method (15.6 nM) [25].

The monitored core mode intensity fluctuates by only about 0.01 dB, indicating that the sensor and sensing system are highly stable and surrounding environmentally-induced effects on the measured results can be ignored.
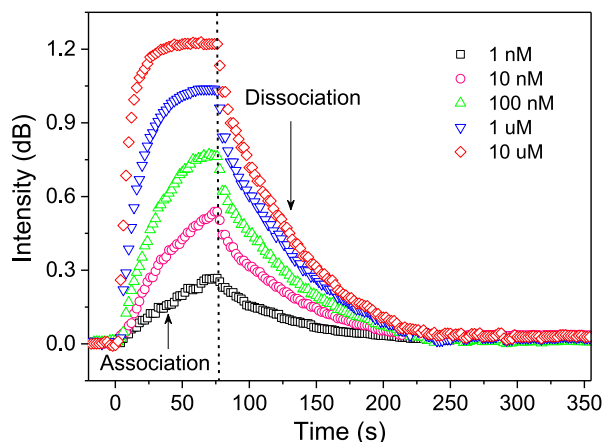

Fig. 8. Real-time interaction of small molecule AdoHcy with protein Set7 in different concentration.

B. Interaction Monitoring

Because of the low volume design of our microfluidic system, our system can be easy used for real-time monitoring of the interaction between AdoHcy and Set7. By selectively injecting buffer or AdoHcy solutions into the sample cell, interactions including association and dissociation between AdoHcy and Set7 can be monitored in real-time. Figure 8 shows the experimental results of this interaction for different AdoHcy concentration levels from 1 nM to 10 μM. As can be seen, when the AdoHcy solution is injected into the sample cell, the intensity change in the selected SPR resonance increases sharply to a saturated level as the AdoHcy concentration increases, agreeing with the theory that the association ratio increases as the concentration arises. When the buffer solution is injected into the sample cell, the AdoHcy bonded to the AdoHcy dissociates from the Set7 due to the decrease in AdoHcy concentration, thus leading to intensity variation decreases. As the buffer solution is continuously injected into the sample cell, the AdoHcy concentration can reach approximately zero, resulting in the intensity variation returning to zero. Except for the action of replacing the injection syringe for injecting biosample solutions of different concentrations into the biosample cell, all operations are automatic, making the implementation of interaction monitoring easy and the system stable. Therefore, biomolecule interaction can be monitored in real-time using our proposed plasmonic TFBG biosensor together with our designed microfluidic system.

Table 1 summarizes the main characteristics of our plasmonic TFBG sensor for AdoHcy detection in comparison with other methods. We can see that our sensor provides an LOD comparable to (even better than) that of recent reported methods. Meanwhile, the proposed sensor requires smaller volume of sample solution (with only 20 μl) and offers a faster response time (12 min). Finally, our sensor demonstrates its ability of quantitative discrimination for the complete association and dissociation process of small biomolecule interactions at a low concentration of 1 nM, opening up a useful tool for real-time and *in-situ* monitoring of the surface affinity of biomolecules binding and interaction actives in micro space.

TABLE 1
SUMMARY OF THE MAIN CHARACTERISTICS OF DIFFERENT AdoHcy SENSORS REPORTED SO FAR

Method	LOD (nM)	Sample volume (μL)	Detected time (min)	Interaction quantification	Reference
Capillary electrophoresis	60.0	3×10^3	15.0	No report	24
ELISA[1]	15.6	1.5×10^3	60.0	Demonstrated	25
Liquid chromatography (MS[2])	6.4	50	12.0	No report	22
Liquid chromatography (ESI-MS[3])	1.0	200	15.7	No report	23
Fiber-optic (TFBG-SPR)	1.0	20	12.0	Demonstrated	This work

[1]ELISA: Enzyme linked immunosorbent assay; [2]MS: Mass spectrometry; [3]ESI-MS: Electrospray ionization tandem mass spectrometry.

V. CONCLUSION

We have proposed and experimentally demonstrated a label-free plasmonic TFBG biosensor with a reflective sensing configuration for detection of small molecule AdoHcy. Through binding the corresponding protein Set7 as bio-receptor over the sensor surface, AdoHcy can be detected in concentrations as low as 1 nM. Furthermore, using a microfluidic injection system, we have also monitored the interaction between AdoHcy and Set7 for different AdoHcy concentrations between 1 nM and 10 μM. The sensing system, including sensing probe and microfluidic system, is simple to fabricate and easy to implement, and it can be used for rapid, label-free, real-time and microliter-volume biomolecule detection together with biomolecule interaction monitoring.

REFERENCES

[1] J. Albert, L. Y. Shao, and C. Caucheteur, "Tilted fiber Bragg grating sensors," *Laser Photon. Rev.*, vol. 7, no. 1, pp. 83–108, 2013.

[2] F. Baldini, M. Brenci, F. Chiavaioli, A. Giannetti, and C. Trono, "Optical fibre gratings as tools for chemical and biochemical sensing," *Analytical Bioanalytical Chem.*, vol. 402, no. 1, pp. 109–116, 2012.

[3] M. I. Zibaii, H. Latifi, A. Asadollahi, and A. H. Bayat, "Label free fiber optic apta-biosensor for in-vitro detection of dopamine," *J. Lightw. Technol.*, vol. 34, no. 19, pp. 4516–4524, Oct. 2016.

[4] X.-D. Wang and O. S. Wolfbeis, "Fiber-optic chemical sensors and biosensors (2008–2012)," *Analytical Chem.*, vol. 85, no. 2, pp. 487–508, 2013.

[5] V. Marquez-Cruz and J. Albert, "High resolution NIR TFBG-assisted biochemical sensors," *J. Lightw. Technol.*, vol. 33, no. 16, pp. 3363–3373, Aug. 2015.

[6] X. Chen, J. Xu, X. Zhang, T. Guo, and B. O. Guan, "Wide range refractive index measurement using a multi-angle tilted fiber Bragg grating," *IEEE Photon. Technol. Lett.*, vol. 29, no. 9, pp. 719–722, May 2017.

[7] L. Fu *et al.*, "High-sensitive and temperature-self-calibrated tilted fiber grating biological sensing probe," *Sci. Bull.*, vol. 58, no. 21, pp. 2611–2615, 2013.

[8] Y. Shevchenko *et al.*, "In situ biosensing with a surface plasmon resonance fiber grating aptasensor," *Analytical Chem.*, vol. 83, no. 18, pp. 7027–34, 2011.

[9] I. M. White and X. Fan, "On the performance quantification of resonant refractive index sensors," *Opt. Express*, vol. 16, no. 2, pp. 1020–1028, 2008.

[10] C. Caucheteur, T. Guo, and J. Albert, "Review of plasmonic fiber optic biochemical sensors: Improving the limit of detection," *Analytical Bioanalytical Chem.*, vol. 407, no. 14, pp. 3883–3897, 2015.

[11] V. Voisin, J. Pilate, P. Damman, P. Mégret, and C. Caucheteur, "Highly sensitive detection of molecular interactions with plasmonic optical fiber grating sensors," *Biosensors Bioelectronics*, vol. 51, no. 2, pp. 249–254, 2014.

[12] S. Lepinay, A. Staff, A. Ianoul, and J. Albert, "Improved detection limits of protein optical fiber biosensors coated with gold nanoparticles," *Biosensors Bioelectronics*, vol. 52, no. 4, pp. 337–344, 2014.

[13] O. Tehlivets, N. Malanovic, M. Visram, T. Pavkov-Keller, and W. Keller, "S-adenosyl-L-homocysteine hydrolase and methylation disorders: Yeast as a model system," *Biochim. Biophys. Acta*, vol. 1832, no. 1, pp. 204–215, 2013.

[14] Z. Luka, S. H. Mudd, and C. Wagner, "Glycine N-methyltransferase and regulation of S-adenosylmethionine levels," *J. Biol. Chem.*, vol. 284, no. 34, pp. 22507–22511, 2009.

[15] R. Castro *et al.*, "Intracellular S-adenosylhomocysteine increased levels are associated with DNA hypomethylation in HUVEC," *J. Mol. Med.*, vol. 83, no. 10, pp. 831–836, 2005.

[16] V. K. C. Ponnaluri, P.-O. Estève, C. I. Ruse, and S. Pradhan, "S-adenosylhomocysteine hydrolase participates in DNA methylation inheritance," *J. Mol. Biol.*, vol. 430, no. 14, pp. 2051–2065, 2018.

[17] R. Castro *et al.*, "Increased homocysteine and S-adenosylhomocysteine concentrations and DNA hypomethylation in vascular disease," *Clin. Chem.*, vol. 49, no. 8, pp. 1292–1296, 2003.

[18] D. M. Kerins, M. J. Koury, A. Capdevila, S. Rana, and C. Wagner, "Plasma S-adenosylhomocysteine is a more sensitive indicator of cardiovascular disease than plasma homocysteine," *Amer. J. Clin. Nutrition*, vol. 74, no. 6, pp. 723–729, 2001.

[19] H. Gellekink, D. van Oppenraaij-Emmerzaal, A. van Rooij, E. A. Struys, M. den Heijer, and H. J. Blom, "Stable-isotope dilution liquid chromatography–electrospray injection tandem mass spectrometry method for fast, selective measurement of S-Adenosylmethionine and S-Adenosylhomocysteine in plasma," *Clin. Chem.*, vol. 51, no. 8, pp. 1487–1492, 2005.

[20] G. Luippold, U. Delabar, D. Kloor, and B. Mühlbauer, "Simultaneous determination of adenosine, S-adenosylhomocysteine and S-adenosylmethionine in biological samples using solid-phase extraction and high-performance liquid chromatography," *J. Chromatography B, Biomed. Sci. Appl.*, vol. 724, no. 2, pp. 231–238, 1999.

[21] S. Taysi *et al.*, "Plasma homocysteine and liver tissue S-adenosylmethionine, S-adenosylhomocysteine status in vitamin B6-deficient rats," *Eur. Rev. Med. Pharmacological Sci.*, vol. 19, no. 1, pp. 154–160, 2015.

[22] R. Rodriguez *et al.*, "Quantification of S-adenosylmethionine and S-adenosylhomocysteine in human placenta and placental explants under homocysteine treatment," *Int. J. Mass Spectrometry*, vol. 421, pp. 279–284, 2017.

[23] E. Arning and T. Bottiglieri, "Quantitation of S-Adenosylmethionine and S-Adenosylhomocysteine in plasma using liquid chromatography-electrospray tandem mass spectrometry," *Methods Mol. Biol.*, vol. 1378, pp. 255–262, 2016.

[24] A. V. Ivanov, B. P. Luzyanin, E. D. Virus, A. S. Rotkina, and A. A. Kubatiev, "Detection of S-adenosylhomocysteine and methylation index in blood by capillary electrophoresis," *Electrophoresis*, vol. 35, no. 20, pp. 2972–2977, 2015.

[25] X. Hao *et al.*, "Immunoassay of S-adenosylmethionine and S-adenosylhomocysteine: The methylation index as a biomarker for disease and health status," *BMC Res. Notes*, vol. 9, no. 1, pp. 498–513, 2016.

[26] X. Chen *et al.*, "Liquid crystal-embedded tilted fiber grating electric field intensity sensor," *J. Lightw. Technol.*, vol. 35, no. 16, pp. 3347–3353, Aug. 2017.

[27] T. Guo, Á. GonzálezVila, M. Loyez, and C. Caucheteur, "Plasmonic optical fiber-grating immunosensing: A review," *Sensors*, vol. 17, no. 12, pp. 2732–2751, 2017.

[28] T. Guo, "Fiber grating-assisted surface plasmon resonance for biochemical and electrochemical sensing," *J. Lightw. Technol.*, vol. 35, no. 16, pp. 3323–3333, Aug. 2017.

[29] L. Han *et al.*, "Specific detection of aquaporin-2 using plasmonic tilted fiber grating sensors," *J. Lightw. Technol.*, vol. 35, no. 16, pp. 3360–3365, Aug. 2017.

Xiaoyong Chen received the B.Sc. degree in optical information science and technology from Beijing Jiaoyong University, Beijing, China, in 2009, and the Ph.D. degree in communication systems and technologies from the Technical University of Madrid, Madrid, Spain, in 2015. Thereafter, he worked as a Postdoctoral Fellow with the Institute of Photonics Technology, Jinan University, Guangzhou, China. In 2017, he joined the Shantou University as a Lecturer. His research interests include fiber-optic sensor, especially its application for biochemical detection, and optical fiber communications.

Yinggang Nan is currently pursuing the Master's degree in optical engineering at the Institute of Photonics Technology, Jinan University, Guangzhou, China. His research interests include plasmonics and optical fiber sensors.

Xuanyue Ma is currently pursuing the Ph.D. degree in biochemistry at the JNU-HKUST Joint Laboratory for Neuroscience and Innovative Drug Research, Jinan University, Guangzhou, China.

Haiyang Liu received the B.Sc. degree in pharmaceutical sciences from Jilin University, Changchun, China, and the Master's and Ph.D. degrees in biochemistry and molecular biology from Peking University, Beijing, China. He is currently a Postdoctoral Fellow with the Shenzhen Peking University–The Hong Kong University of Science and Technology Medical Center, Shenzhen, China.

Wei Liu received the Ph.D. degree from the Hong Kong University of Science and Technology, Clear Water Bay, Hong Kong, in 2011. He is currently a Professor with the Shenzhen Peking University–The Hong Kong University of Science and Technology Medical Center, Shenzhen, China. He is the Principal Investigator of three grants from the National Natural Science Foundation of China, two from the Shenzhen Basic Research Grant, and one from the Natural Science Foundation of Guangdong Province. His publications included papers in *Cell*, *eLife*, *Structure*, *Journal of Biological Chemistry, Biochemical and Biophysical Research Communications*, etc. In 2012, he won the Young Scientist Award of Hong Kong Institute of Science.

Lei Shi received the B.Sc. and Ph.D. degrees in biochemistry from the Hong Kong University of Science and Technology, Clear Water Bay, Hong Kong, in 2004 and 2009, respectively. In 2011, she joined the Jinan University, Guangzhou, China as an Associate Professor, and was promoted to a Full Professor in 2015. She is the Principal Investigator of the JNU-HKUST Joint Laboratory for Neuroscience and Innovative Drug Research, Jinan University, Guangzhou, China. Her publications included papers in *Proceedings of the National Academy of Sciences of the United States of America*, *Nature Neuroscience*, *Neuron*, *Trends in Neurosciences*, etc. Her research interests include the molecular mechanisms that govern neuronal differentiation, morphogenesis, and function in both normal brain development and diseased conditions, such as Autism spectrum disorder, Alzheimer's disease, and hypoxic-ischemic brain damage.

Tuan Guo received the B.Sc. and the M.Sc. degrees in electrical engineering from Xi'an Shiyou University, Xi'an, China, in 2001 and 2004, respectively, and the Ph.D. degree in optics from Nankai University, Tianjin, China, in 2007. Thereafter, he worked as a Postdoctoral Fellow with the Department of Electronics at Carleton University, Ottawa, ON, Canada, and with the Photonics Research Centre, The Hong Kong Polytechnic University, Hung Hom, Hong Kong. In 2011, he joined the Jinan University, Guangzhou, China as an Associate Professor, and was promoted to a Full Professor in 2014. He has authored more than 200 papers in peer-reviewed international journals (including *Nature Communications*, *Light: Science & Applications*, and six tutorial/invited reviews), one Springer Handbook in chapters, and presented over 30 invited talks at international conferences. He holds 20 patents and pending patents. His research interests include optical fiber sensors, fiber gratings, plasmonics, biophotonics, and photonics for renewable energy. He was a Co-Chair of the IEEE-IMS Technical Committee "Photonic Technology in Instrumentation and Measurement" and is a Senior Member of the Optical Society of America (OSA). He was a Guest Editor for IEEE/OSA *Journal of Lightwave Technology*, a Guest Editor for MDPI *Sensors*, an Associated Editor for *Journal of Sensors*, the Technical Program Committee Co-Chair of the 13th Pacific Rim Conference on Lasers and Electro-Optics (CLEO-PR 2018, Hong Kong, China), and Special Session Chair of the 33rd IEEE International Instrumentation and Measurement Technology Conference (I^{2}MTC 2018, Houston, USA).